CHAPTER 5

The Effect of Thyroid Hormone Receptor Truncating Mutants on Gene Transcription in Neuronal Cells

Karn Wejaphikul, W. Edward Visser, Selmar Leeuwenburgh, Wilfred F.J. van IJcken, Robin P. Peeters, Marcel E. Meima

Manuscript in preparation

http://hdl.handle.net/1765/119488

5

Abstract

Thyroid hormone receptor (TR) α1 is the predominant TR isoform in the brain and plays a vital role in neurodevelopment. Mutations in TRα1 that reduce or abolish T3 binding to the receptor are the cause of the syndrome of resistance to thyroid hormone alpha (RTHα), which is characterized among others by motor and cognitive impairment in RTHα patients. Although a genotype-phenotype relation has been reported, it is clear that the severity of the neurological phenotype does not always correlate with the degree of T3 binding impairment of mutant receptors. However, the mechanism underlying this phenotypic difference is unclear. To understand the differences of the neurological phenotype in RTHα patients, we analyzed gene regulation by two TRα1 truncating mutations, C380fsx387 and F397fsx406, both of which exhibited negligible T3 binding but create a different degree of cognitive impairment in patients. RNA was extracted from human-derived neuronal (SH-SY5Y) cells stably expressing FLAG-HA-tagged (FH) wild-type (WT) or mutant TRα1 after stimulation with vehicle or 10 nM T3. Transcriptomes were analyzed by RNA sequencing. The results showed that, in contrast to WT, cells expressing the mutant receptors lacked any T3-induced gene expression. Unstimulated gene expression was also different in cell expressing mutant versus WT receptors. This difference was more pronounced in FHTRα1-C380fsx387 than in -F397fsx406 expressing cells, indicating a differential effect of these mutants on baseline gene expression. Many genes that are specifically dysregulated by FHTRα1-C380fsx387 but not -F397fsx406 compared to both WT are involved in the nervous system development and neuronal migration. These findings may explain the more severe neurological phenotype found in the patient carrying the C380fsx387-TRα1 mutation.

Introduction

Thyroid hormone (TH) is indispensable for proper neurodevelopment. Impaired TH action during brain development can lead to various degrees of psychomotor retardation and neurological impairment (1-3). The genomic actions of TH are regulated by thyroid hormone receptors (TRs). The TR isoform α1 (TRα1) is broadly expressed in the brain and is considered the major isoform to be involved in brain development (4-7).

Mutations in the ligand binding domain (LBD) of TRα1 cause resistance to thyroid hormone alpha (RTHα). The clinical phenotype of RTHα patients includes growth retardation, macrocephaly, constipation, and anemia (8-10). Patients also present with neurodevelopmental defects, including cognitive and motor impairment, autistic spectrum disorder (ASD), and epilepsy (8,11), confirming the importance of TRα1 for a proper brain development. To date, 25 mutations (in a total of 40 patients) have been identified as a cause of RTHα. These mutations can be categorized into two groups. The first group consists of truncating mutations that create premature stop codons and shorten the length of the LBD. These mutations abolish the T3 binding affinity and T3-induced transcriptional activity of TRα1 (12-19). The second group consists of missense mutations that result in single amino acid substitutions in the LBD. These mutants bind T3 but with a lower affinity than wild-type (WT) receptors (8,15,17,20-27).

The neurological phenotype of patients with truncating mutations is generally more severe than that of patients with missense mutations (8). Interestingly, there is also a striking diversity in the severity of the neurological phenotype within the group of patients carrying truncating mutations. For instance, patients with a TRα1-F397fsx406 mutation have a relative mild neurological phenotype with borderline cognitive and motor impairment (IQ score 90) (13,14), whereas the patients with a TRα1-C380fsx387 and -A382fsx388 mutations have severe mental retardation (TRα1-C380fsx387 patient was unable to walk and communicate at 12 years of age and TRα1-A382fsx388 patient has IQ score 52) (16,17). Since all TRα1 truncating mutants exhibited negligible T3 binding (13,17), other mechanisms than impaired T3-affinity must be involved that are causing this differences in the neurocognitive phenotype.

In order to better understand the diversity of neurocognitive impairment of RTHα patients carrying truncating mutations, we studied the pattern of neuronal gene expression regulated by WT TRα1 and two truncating TRα1 mutants (C380fsx387 and F397fsx406) of patients with two very distinct neurocognitive phenotypes.

Materials and Methods

Plasmid constructs

A lentiviral bicistronic vector to drive expression of N-terminal FLAG and Hemagglutinin (HA) tagged (FH) WT human TRα1 together with the puromycin resistance marker, and green fluorescent protein (GFP) (pLentiFHTRα1 WT) was created as previously described (Chapter 6a). The TRα1-C380fsx387 (pLentiFHTRα1-C380fsx387) or -F397fsx406 (pLentiFHTRα1-F397fsx406) mutations were generated using the Quik Change II kit according to the manufacturer's protocol (Agilent Technologies, Amstelveen, The Netherlands). An empty vector (EV; pLentiMCS) expressing only the puromycin resistance marker and GFP was used to create an EV control cell line. The pMD2.G and psPAX2 packaging vectors (Chapter 6a) were used to produce lentiviruses in 293FT cells. The pdV-L1 luciferase-renilla reporter construct containing the luciferase reporter gene under control of a thyroid hormone response element (TRE) (22) was used to study the T3-induced transcriptional activity of TRs in TR-expressing cell lines.

Stable expression of TRs in SH-SY5Y cells

Lentivirus production and viral transduction have been previously described (Chapter 6a). Briefly, lentiviruses containing pLentiFHTRα1 WT, pLentiFHTRα1-C380fsx387, pLentiFHTRα1-F397fsx406, and pLentiMCS were produced in 293FT cells seeded in 10 cm tissue culture dishes by co-transfecting 4 µg of lentiviral constructs with 4 µg of psPAX2 and pMD2.G plasmids using Xtreme Gene 9 transfection reagent according to the manufacturer's protocol (Roche Diagnostics, Almere, NL). SH-SY5Y cells were grown in 6-well plate using growth medium (DMEM/F12 supplemented with 9%FBS, 100 U/mL penicillin, 100 µg/mL streptomycin, 100 nM Na_2SeO_3) and infected with lentivirus at 25% confluency. After 48 hours, infected cells were selected with 2 µg/mL of puromycin. Puromycin-resistant SH-SY5Y cells (SH-SY5Y/FHTRα1 WT, -C380fsx387, -F397fsx406, and MCS) were expanded in selection medium (growth medium supplemented with 2 µg/mL puromycin). After two passages, cells were subcultured at a 1:10,000 dilution ratio into 10 cm culture dishes in order to growth of separate clones. The clones were selected and screened for TR expression by immunoblotting before expanding for subsequent experiments.

Immunoblotting

The expression of FH-TRα1 WT and mutants in monoclonal SH-SY5Y cells was verified by immunoblotting of nuclear extracts (NEs) as previously described (22,28), using 1:1,000 dilution of a HA-Tag antibody (C29F4) Rabbit mAb (#3724, Cell Signaling Technology, Leiden, NL). Histone 3 protein was detected as a loading control using a 1:1,000 dilution of a Histone 3 (H3; 1B1B2) antibody (#14269, Cell Signaling Technology, Leiden, NL).

Transfection and luciferase assays

T3-induced transcriptional activity of FH-TRα1 WT and mutants in monoclonal SH-SY5Y cells was determined by transfecting 200 ng of the pdV-L1 luciferase-renilla reporter construct into cells at 80% confluency in 24-wells tissue culture plates in TH-depleted medium (DMEM/F12 supplemented 9% charcoal-treated FBS) using Xtreme Gene 9 transfection reagent (Roche Diagnostics, Almere, NL) according to the manufacturer's protocol. After 24 hours transfection, cells were stimulated with 0-1,000 nM T3 for 24 hours in DMEM/F12 supplemented with 0.1% bovine serum albumin (BSA). Luciferase and renilla activities in cell lysates were measured as previously described (13) using the Dual Glo Luciferase kit (Promega, Leiden, NL). The luciferase to renilla ratio was calculated to adjust for transfection efficiency and was shown as mean ± standard error of the mean (SEM) of four independent experiments performed in triplicate.

T3 stimulation and RNA isolation for transcriptome analysis and qRT-PCR

The monoclonal transduced SH-SY5Y cells were plated in 6-well culture plates in selection medium. At 80% confluency, the cells were cultured for 24 hours in DMEM/F12 supplemented with 9% charcoal-stripped FBS to deplete TH and subsequently stimulated for 6 hours with 0 or 10 nM T3 in DMEM/F12 supplemented with 0.1% BSA. RNA was then isolated from the cells using Trizol reagent (TRI Reagent®, Sigma-Aldrich, Zwijndrecht, NL) and further purified with EchoCLEAN RNA CleanUp kit (020-002-050-050, BioEcho, Cologne, Germany), according to the manufacturer's protocol. RNA samples of three independent experiments performed in triplicate for each receptor and T3 concentration were collected. One sample of each triplicate was sent for RNA sequencing, and the other two samples were used for qRT-PCR.

Next-generation RNA sequencing (RNA-seq)

Purity and quality of isolated RNA were assessed by Agilent 2100 Bioanalyzer (Agilent Technologies, Santa Clara, CA). The RNA was prepped with the Illumina TruSeq Stranded mRNA Library Prep Kit (Illumina, Eindhoven, NL). The resulting DNA libraries were sequenced according to the Illumina TruSeq Rapid v2 protocol on an Illumina HiSeq2500 sequencer. Reads were generated of 50 base-pairs in length. Subsequently, adapter sequences were trimmed off, and the trimmed reads were matched against the requested reference (GRCh38 version of the human reference genome) using HiSat2 (version 2.1.0). Gene expression values were called using HTseq-count (version 0.9.1).

Differential gene expression analysis

Gene expression values from HTseq-count were analyzed using the R program. Read counts were first normalized with the DEseq2 package from R (29) and filtered for genes that had a false discovery rate (FDR) above 0.05 and low normalized count (<10 reads in

more than 21 samples). Principle component analysis (PCA) and pairwise distance heat map were performed to visualize the clustering of the samples. Pairwise comparisons of differential expression were determined using the DEseq2 package from R (29). A p-value adjusted for multiple comparisons < 0.05 was considered significant. Subset of genes that have at least a 4-fold difference in expression (log2 fold change ≥ ±2) for each pairwise comparison was defined as highly differentially expressed genes (H-DE genes). Gene Ontology terms (molecular function, MF; biological process, BP; cellular component, CC) enrichment analysis was performed by DAVID functional annotation chart (DAVID Bioinformatics Resources 6.8, NIAID/NIH: https://david.ncifcrf.gov/) using default setting (count 2, ease 0.1). Statistical significance was considered when p-values of modified Fisher's exact test (EASE score) with Benjamini post-test < 0.05.

Quantitative real-time polymerase chain reaction (qRT-PCR)

RNA was reverse transcribed using the transcriptor high fidelity cDNA synthesis kit (05091248001, Roche Diagnostics, Almere, NL) according to the manufacturer's protocols. qRT-PCR was performed on 25 ng cDNA using TaqMan probes for KLF9 (Hs00230918_m1), HR (Hairless) (Hs00218222_m1), and Cyclophilin A (Cat. No. 4310883E, ThermoFisher Scientific, Landsmeer, NL), and qPCR Core kit for SYBR® Green (Eurogentec, Maastrich, NL) with *GAPDH* (forward primer: 5'-GAGTCCTTCCACGATACCAAAG-3', reverse primer: 5'-GGTGTGAACCATGAGAAGTATGA-3') and *THRA* (forward primer: 5'-AGACCAGATCATCCTCCTGAA-3', reverse primer: 5'-CCGCTTGACAGCCATCTC-3') primers. The expression of *KLF9*, *HR* and *THRA* were quantified by the ddCt method using the geometric means of two house-keeping genes (Cyclophilin A and GAPDH) expression for normalization. Data are presented as mean ± SEM of three independent experiments performed in duplicate.

Results

Expression and transcriptional activity of FH-TRα1 WT and mutants in SH-SY5Y cells

To study the effect of TRα1 truncating mutations on gene expression in neuronal cells, we introduced WT TRα1 and two truncating mutants, C380fsx387 and F397fsx406, into SH-SY5Y cells using lentiviral transduction. Monoclonal cell strains were selected to get a genetically homogenous and clonal population. The mRNA expression of *THRA* in all three TRα1 expressing cell lines was substantially higher than the MCS control cells (approximately 100-fold for SH-SY5Y/FHTRα1 WT, 60-fold for -C380fsx387, and 90-fold for -F397fsx406 cells), confirming a low level of endogenous TRα1 expression in SH-SY5Y cells and the success of FH-TRα1 transduction (Supplementary Figure S1A). Immunoblots of NEs

from SH-SY5Y cells confirmed that all three FHTRα1 are efficiently expressed in the cells, albeit with slightly lower expression levels for FHTRα1-C380fsx387 than for FHTRα1 WT and FHTRα1-F397fsx406 (Supplementary Figure S1B). WT TRα1 showed normal T3-induced transcriptional activity in luciferase assays (Supplementary Figure S1C). In contrast, the two truncating mutants showed no response to T3-stimulation at any of the concentrations tested, indicating a complete loss of T3-induced transcriptional activity for these mutants.

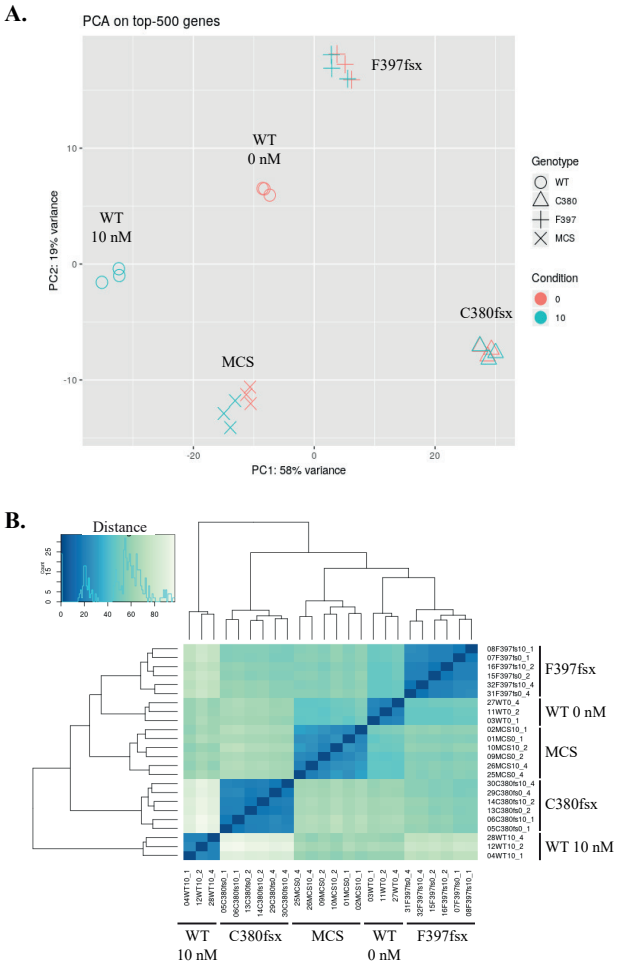

Figure 1. (A) Principal component analysis (PCA) of the top 500 genes of RNA sequencing data from SH-SY5Y/FHTRα1 WT, -C380fsx387, -F397fsx406, and MCS control cells (after 6 hours 0 or 10 nM T3 stimulation) clearly demonstrates the clustering of biological replicates from a similar TR and T3 condition. The samples from cells expressing WT receptor are separated into two clusters, depending on the T3 concentration. In contrast, samples from cells stimulated by 0 and 10 nM T3 are clustered together in MCS control and the two mutants, suggesting a small effect of T3 on their transcriptomes. (B) The heatmap illustrates the pairwise distance between samples clustered by hierarchical clustering analysis. The key color on the top left indicates the distances between samples. In agreement with the PCA plot, samples from the same cell type and T3 condition are clustered together.

Overall gene expression

RNA sequencing was performed to evaluate the different patterns of gene expression elicited by WT and the two TRα1 truncating mutants in SH-SY5Y cells. At least 23 million reads were generated for each sample, and more than 95% of these reads were aligned with the reference sequence. After normalization and filtering, 17,788 genes remained for analysis. The PCA plot and pairwise distance heat map showed a high degree of clustering of the three biological replicates for each TR and T3 condition (Figure 1). The cluster of T3-stimulated SH-SY5Y/FHTRα1 WT was separated from unstimulated WT (0 nM T3), indicating global changes in the pattern of gene expression elicited by the liganded WT TRα1. In contrast, the six biological replicates of the SH-SY5Y/FHTRα1-C380fsx387 and -F397fsx406 were clustered together, regardless of T3, indicating that these two mutants did not respond to T3. The fold increase in RNA reads of two known TH responsive genes, *KLF9* and *HR*, were similar to the results of qPCR (independent samples) (Supplementary Figure S2), confirming the reliability of the RNA sequencing.

We then analyzed the effect of 10 nM T3 stimulation on gene expression of each cell line. The relatively short 6-hour T3 incubation was chosen to minimize the chance that differentially expressed genes were not directly controlled by T3-TRα1 but rather secondarily via a T3-induced transcription factor (30-32). The results showed that, in the presence of WT TRα1, the expression of 5,688 genes was significantly changed by 10 nM T3 (2,999 T3-upregulated genes and 2,689 T3-downregulated genes) (Figure 2). In contrast, only 43 genes were differentially expressed between unstimulated and 10 nM T3 stimulated in the MCS control group. In SH-SY5Y/FHTRα1-C380fsx387 or -F397fsx406 cells, T3 did not significantly alter the expression of any gene.

Since T3 did not affect the pattern of gene expression in SH-SY5Y/FHTRα1-C380fsx387 and -F397fsx406 cells, we from here on only focused on unstimulated gene expression to study the difference between the two mutants. The expression heat map showed that the overall pattern of unstimulated gene expression of the SH-SY5Y/FHTRα1-F397fsx406 cells was more similar to WT than to -C380fsx387 cells (Figure 2). We set stringent criteria of a minimal 4-fold difference in gene expression levels, designated highly differentially expressed (H-DE) genes, to ensure that the differences are likely to have a biological impact. The number of H-DE genes between unstimulated SH-SY5Y/FHTRα1-F397fsx406 and WT cells was also much smaller than between unstimulated SH-SY5Y/FHTRα1-C380fsx387 and WT cells (Figure 3), confirming that the C380fsx387 mutant creates a more distinct pattern of baseline gene expression compared to WT than the F397fsx406 mutant.

Differential gene expression of FHTRα1-C380fsx387 versus -F397fsx406

We performed pairwise comparison to determine which genes are differentially expressed between unstimulated SH-SY5Y/FHTRα1-C380fsx387 and -F397fsx406 cells. Overall, 4,629 genes were differentially expressed between the two cell lines, of which 721

were H-DE genes. Of those, 342 genes were T3 responsive genes, i.e., genes that had a significantly different expression level after 10 nM T3 stimulation in the WT cells (Figure 4A).

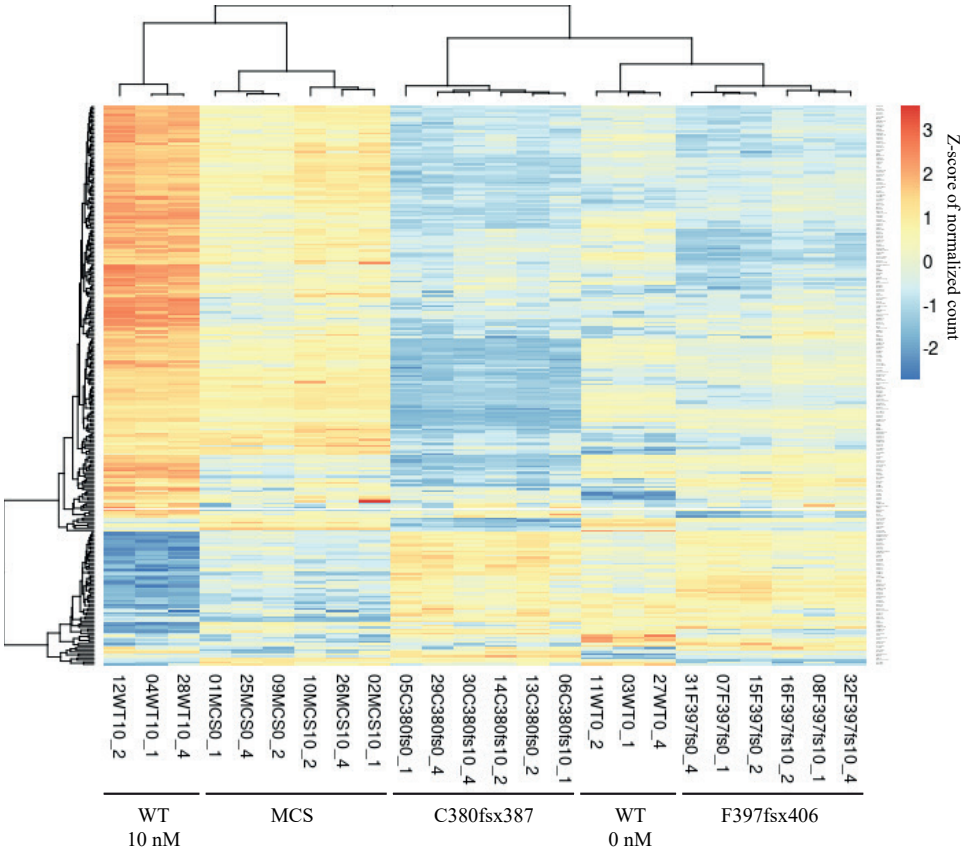

Figure 2. The expression heat map of the normalized RNA sequencing data illustrates the pattern of gene expression of all samples. Data are shown as a Z-score of normalized counts per gene (key color on the right). The dendrogram shows hierarchical clustering of genes (row) and samples (column) (analyzed by average linkage clustering and Pearson distance measurement methods). The heat map is clearly different between unstimulated and 10 nM T3 stimulation in WT cells. In contrast, there is no clear difference in the heat map of SH-SY5Y/FHTRα1-C380fsx387 and -F397fsx406 cells after 10 nM T3 stimulation (all samples are clustered together). In addition, the heat map of SH-SY5Y/FHTRα1-F397fsx406 cells is more similar to unstimulated WT than that of -C380fsx387 cells, suggesting a stronger effect of the C380fsx387 mutation than the F397fsx406 mutation on gene expression of unstimulated cells.

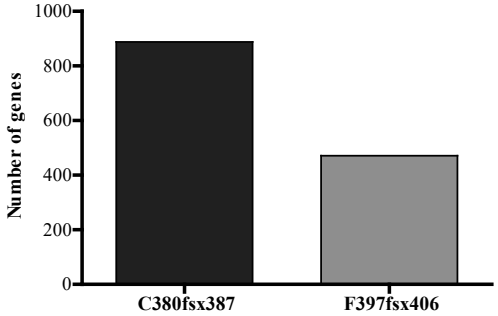

Figure 3. The bar chart shows number of H-DE genes between unstimulated SH-SY5Y/FHTRα1-C380fsx387 and WT cells (888 genes, black bar) and between SH-SY5Y/FHTRα1-F397fsx406 and WT cells (471 genes, grey bar).

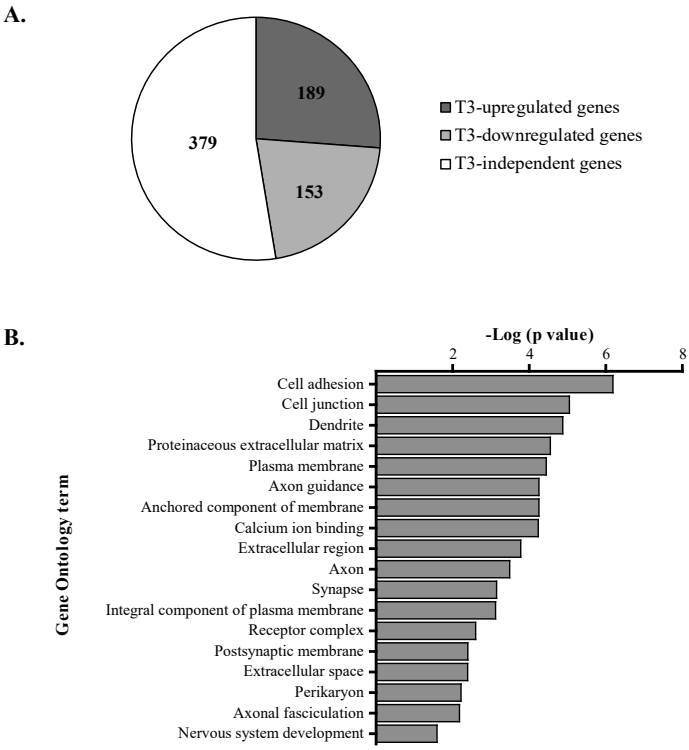

Figure 4. 721 H-DE genes between unstimulated SH-SY5Y/FHTRα1-C380fsx387 and -F397fsx406 cells. (A) Pie chart shows that 342 genes (47%) are T3-responsive genes, i.e., genes that had a significantly different expression level after 10 nM T3 stimulation in the WT cells (189 genes are T3-upregulated and 153 genes are T3-downregulated), whereas 379 genes (53%) are T3-independent (the expression level does not change after 10 nM T3 stimulation). (B) The result of the gene ontology (GO) enrichment analysis showed that the genes were significantly enriched (Benjamini p value < 0.05) with 18 GO terms, most of which are related to the physiology of neurons.

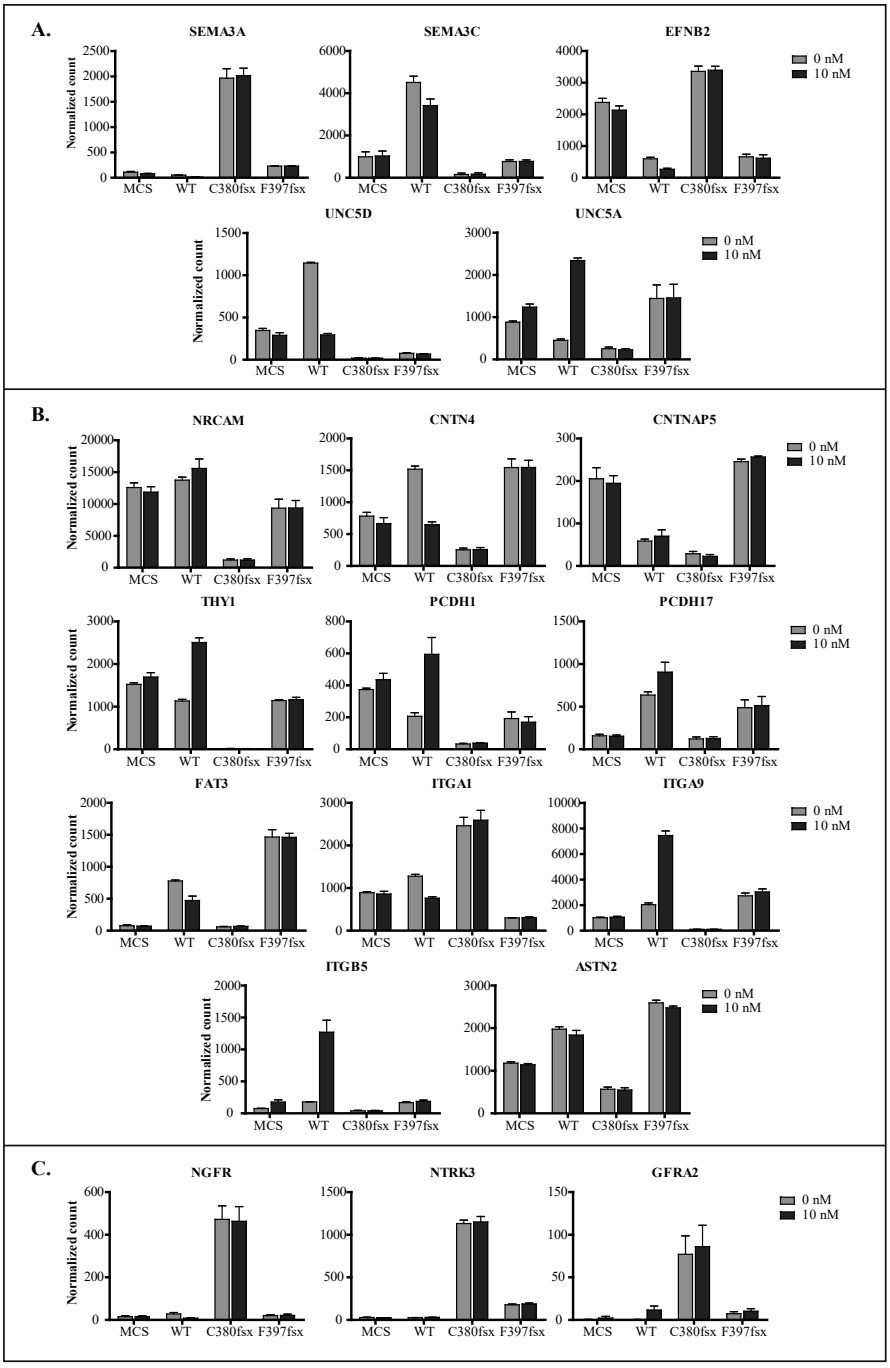

Figure 5. Expression of selected individual genes that are significantly enriched for at least one GO term. These genes encode (A) neuronal guidance molecules, (B) cell adhesion molecules, and (C) neurotrophic factors, which play an important role in nervous system development and neuronal growth and migration. (Data are shown as mean ± SEM of three biological replicates of normalized count from RNA sequencing.)

Gene ontology (GO) enrichment analysis of FHTRα1-C380fsx387 highly differential genes

Next, we analyzed whether the H-DE genes between unstimulated SH-SY5Y/FHTRα1-C380fsx387 and -F397fsx406 cells were associated with specific GO terms. The result showed that 328 genes were significantly enriched for at least one GO term. The genes were enriched for 18 terms, including one molecular function, four biological processes, and thirteen cellular components, most of which are related to the physiology of neurons (Figure 4B and Table 1). Many genes that significantly enriched with these GO terms encode neuronal guidance molecules, cell adhesion molecules, and neurotrophic factors, which play important roles in nervous system development and neuronal growth and migration (Figure 5 and Table 2). Interestingly, in addition to the genes that were enriched, the expression of two genes that are vital for neuronal differentiation, *ASCL1* and *NEUROG2*, was also remarkably different between SH-SY5Y/FHTRα1-C380fsx387 and SH-SY5Y/FHTRα1 WT or -F397fsx406 (Figure 6 and Table 2).

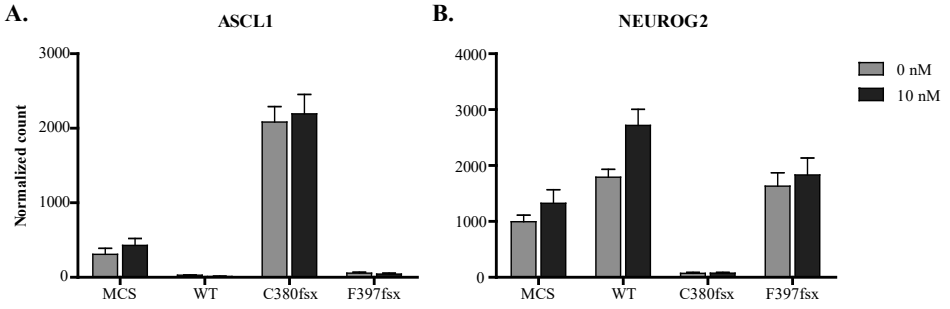

Figure 6. The disparate expression of (A) *ASCL1* and (B) *NEUROG2* in SH-SY5Y/FHTRα1-C380fsx387 cells compared to the SH-SY5Y/FHTRα1 WT and -F397fsx406 cells. (Data are shown as mean ± SEM of three biological replicates of normalized count from RNA sequencing.)

Table 1. Significant Gene Ontology enrichment analysis by DAVID Bioinformatics Resources 6.8, NIAID/NIH (https://david.ncifcrf.gov/).

GO term	Gene list	Fold enrichment	FDR	Benjamini p value
Biological Process (BP)				
Axonal fasciculation (GO:0007413)	CNR1, CNTN2, CNTN4, CRTAC1, NDN, NRCAM, SEMA3A	13.1	0.015	0.007
Axon guidance (GO:0007411)	ANOS1, CNTN2, CNTN4, EFNB2, EPHA8, FEZ1, GFRA3, LGI1, NGFR, NR4A3, NTN4, RELN, SEMA3A, SEMA3C, SLIT1, SLIT2, TENM2, TGFB2, TNR, UNC5A, UNC5D	4.46	<0.001	<0.001
Cell adhesion (GO:0007155)	ADAM12, ADGRE2, ADGRE5, AJAP1, ANOS1, AZGP1, CD9, CNTN2, CNTN4,CNTN6, CNTNAP4, CNTNAP5, COL6A3, EDIL3, EFNB2, ENG, EPHA8, FEZ1, FREM2, ISLR, ITGA8, ITGA9, ITGB5, JCAD, KITLG, LPP, MYBPC2, NLGN4X, NTM, PCDH17, PRKCA, PTPRK, PTPRT, RELN, SIRPA, SORBS2, SPOCK1, SPON1, SSPO, THY1, TNFAIP6, TNR	3.09	<0.001	<0.001
Nervous system development (GO:000739)	CNTN4, CSGAL, NACT1, ENC1, FEZ1, FOS, FUT9, GFRA1, GFRA2, GFRA3, HES4, ITM2A, JAG1, LGI1, MAB21L2, MAFB, MPPED2, NDN, PCDH1, RGS9, SOX14, SPOCK1, ST8SIA4, ZIC5	2.71	0.080	0.025
Molecular Function (MF)				
Calcium ion binding (GO:0005509)	ADGRE2, ADGRE5, ASTN2, CACNA1E, CAPN13, CCBE1, CPS1, CRTAC1, DGKB, DGKG, EDIL3, EYS, FAT3, FBLN2, FSTL4, GUCA1A, HPCAL4, JAG1, KCNIP1, LRP1B, LRP4, MATN3, MCTP1, MCTP2, ME1, MMP17, NID1, PCDH1, PCDH17, PCDHGB7, PHF24, PLA2G4A, PRRG1, RPH3A, S100A10, S100A11, SCGN, SLIT1, SLIT2, SMOC1, SNCB, SPOCK1, SPOCK3, SYT17, SYT2, SYT4, TENM2, TLL2	2.35	<0.001	<0.001
Cellular Component (CC)				
Anchored component of membrane (GO:0031225)	ART4, CD177, CNTN2, CNTN4, CNTN6, GFRA1, GFRA2, GFRA3, GPC5, LYPD1, LYPD6B, MMP17, NT5E, NTM, PRNP, TFPI	4.92	0.001	<0.001
Axon (GO:0030424)	CNR1, CNTN4, COBL, FEZ1, GRIK3, HTR2A, IGF2BP1, IRX3, KCNA2, KCNA3, KCNB1, KIF21B, MME, NEFL, NEFM, PRSS12, PTPRK, SEMA3A, STMN4, SYT4, TGFB2	3.29	0.009	<0.001
Cell junction (GO:0030054)	CADPS, CAMK2N1, CBLN4, CNTNAP4, CXCR4, DACT1, FAIM2, GABRA5, GABRB1, GABRB3, GABRG3, GCOM1, GRIA2, GRIA3, GRIK3, GRIK4, GRIK5, KCNA2, KCNB1, LGI1, LRRC7, LRRTM3, MYZAP, NLGN4X, PRIMA1, RIMS3, RPH3A, SDK2, SIPA1L1, STXBP5, SV2B, SYN3, SYNPR, SYT2, SYT4, TENM2, TMEM163, TRIM9	2.80	<0.001	<0.001

GO term	Gene list	Fold enrichment	FDR	Benjamini p value
Dendrite (GO:0030425)	BRINP2, BRINP3, CAMK2N1, CNTNAP4, COBL, FEZ1, GABRA5, GABRB1, GNG3, GRIK3, GRIK5, HTR2A, KCNA2, KCNB1, KCNIP1, KIF21B, LRP4, MME, NLGN4X, P2RY1, PRSS12, PSD2, PTPRK, RELN, SEMA3A, SLC32A1, SYT4, TENM2, THY1, TRIM9, ZNF385A	3.22	<0.001	<0.001
Extracellular region (GO:0005576)	A2M, ADAM12, ADAMTS3, ADAMTS5, ALKAL2, ANOS1, AOAH, APLN, APOL4, AZGP1, BCHE, BRINP2, BRINP3, C1orf54, C1QTNF1, C6, C7, CLUL1, CNTN4, COL14A1, COL24A1, COL2A1, COL6A3, COLEC11, DBH, DMBT1, FAM19A5, FBLN2, FGF22, FGF7, FSTL4, GPC5, GREM2, IGFBP3, IL13RA2, INHBE, ISLR, JAG1, KITLG, KNG1, LGI1, LYPD1, MATN3, MR1, NGFR, NID1, NPY, NRCAM, NRG3, NTN4, NTS, NXPH1, OAS1, OTOR, PRRG1, PTX3, RBP3, RSPO4, SCGN, SEMA3A, SERPINA5, SLIT1, SLIT2, SUSD4, TAC3, TFPI, TGFB2, TIMP3, TLL2, TNFRSF1A, TNR, TUBA4A, TULP2, VEGFD, VIP, VSTM2A, WNT11, WNT16, XYLT1	1.71	0.004	<0.001
Extracellular space (GO:0005615)	ADAMTS3, ADAMTS5, ADGRE5, ANGPTL2, ANOS1, APLN, APOL4, AZGP1, C1QTNF1 ,CBLN4, CCBE1, CD9, COL14A1, COL2A1, COL6A3, CPB1, CPNE9, DBH, DMBT1, ENG, FGF22, GLDN, GPC5, GREM2, GSDMD, HIST1H2BF, IGFBP3, IL13RA2, INHBE, KIT, KITLG, KNG1, LGI1, NLGN4X, NPY, NRG3, PTGIS, PTX3, RBP3, RELN, S100A11, SEMA3A, SEMA3C, SERPINA5, SERPINB6, SEZ6, SLIT1, SLIT2, SPINK13, SPOCK1, SPOCK3, SPON1, SSPO, TAC3, TFPI, TGFA, TGFB2, TIMP3, TNFAIP6, TNFRSF1A, VEGFD, WNT11, WNT16	1.63	0.196	0.004
Integral component of plasma membrane (GO:0005887)	ABCB4, ABCG1, ADGRE5, AGTR1, APCDD1, AQP10, AQP3, ASIC1, C1QTNF1, CACNB2, CALCRL, CALY, CD9, CNR1, CNTN2, EFNB2, EPHA8, ESYT3, GABRA5, GABRB1, GABRB3, GPC5, GPR1, GRIA2, GRIK3, GRIK4, HAS2, HTR2A, INSRR, JAG1, KCNA2, KCNJ9, KCNK3, KCNK9, LIFR, MME, MMP17, NGFR, NLGN4X, NRCAM, NRG3, NTRK3, P2RX3, P2RY1, PCDH1, PLPPR4, PLPPR5, PLXNA2, PRKD1, PROKR2, PRRG1, PTGER2, PTH1R, PTPRK, RHBG, SLC18B1, SLC6A16, SLC7A14, SLITRK6, SSTR1, TENM2, TGFA, THY1, TLR1, TNFRSF1A, TRHDE, TSPAN2, TSPAN8, VIPR1	1.70	0.024	<0.001
Perikaryon (GO:0043204)	ASS1, ASTN1, ASTN2, GRIK3, GRIK5, ITGA1, ITGA8, KCNA2, KCNAB1, KCNB1, NDN, TMEM100	3.94	0.316	0.006
Proteinaceous extracellular matrix (GO:0005578)	ADAMTS16, ADAMTS3, ADAMTS5, ANOS1, CCBE1, COL14A1, COL24A1, COL6A3, CRTAC1, FBLN2, GLDN, GPC5, MATN3, MMP17, RELN, SLIT1, SLIT2, SMOC1, SPOCK1, SPOCK3, SPON1, TFPI2, TIMP3, TNR, WNT11, WNT16	3.37	<0.001	<0.001

GO term	Gene list	Fold enrichment	FDR	Benjamini p value
Postsynaptic membrane (GO:0045211)	CAMK2N1, FAIM2, GABRA5, GABRB1, GABRB3, GABRG3, GRIA2, GRIA3, GRIK3, GRIK4, GRIK5, KCNB1, LRRC7, LRRTM3, NLGN4X, P2RY1, SIPA1L1, TENM2	2.97	0.177	0.004
Plasma membrane (GO:0005886)	ABCB1, ABCB4, ABCG1, ABCG4, ADAM12, ADCY8, ADGRE2, ADGRE5, AGTR1, ANO3, ANOS1, AQP10, AQP3, ARHGEF28, ART4, ASIC1, ATP10A, AZGP1, BAMBI, CA14, CACNA1E, CACNA1G, CACNB2, CACNG2, CALCRL, CARD11, CD177, CD9, CERK, CNR1, CNTN2, CNTN4, CNTN6, COBL, COLEC12, CSMD2, CXCR4, DGKB, DGKG, DGKK, DOCK5, EFNB2, ELMO1, EPHA8, FAM155B, FAM84B, FAT3, FEZ1, FGFRL1, FREM2, GABRA5, GABRB1, GABRB3, GABRG3, GFRA1, GFRA2, GFRA3, GLDN, GLP1R, GNG3, GPBAR1, GPC5, GPR160, GPR37L1, GRIA2, GRIA3, GRIK3, GRIK4, GRIK5, GSDMD, GUCA1A, HEPH, HTR2A, IFNLR1, ITGA1, ITGA8, ITGA9, ITGB5, ITM2A, JAG1, KCNA2, KCNA3, KCNAB1, KCNB1, KCNIP1, KCNJ3, KCNJ9, KCNK3, KCNK9, KCNN3, KCNQ3, KIRREL1, KIT, KITLG, KNG1, LIFR, LPP, LYPD1, LYPD6B, ME1, MME, MR1, MYOF, NFATC2, NGFR, NLGN4X, NRCAM, NT5E, NTM, NTN4, P2RX3, P2RY1, PANX2, PCDH1, PCDH17, PCDHGB7, PHACTR2, PIK3AP1, PLCE1, PLPPR4, PLPPR5, PLXNA2, PRIMA1, PRKCA, PRKD1, PRNP, PROKR2, PRSS12, PTGER2, PTH1R, PTPRT, PYGL, RAP1GAP2, RELN, RGS9, RHBG, RPH3A, SCN1A, SDK2, SEZ6, SGK1, SHB, SIRPA, SLC27A6, SLC32A1, SLIT2, SSTR1, STXBP5, SV2B, SYT17, SYT2, SYT4, TBC1D30, TENM2, TFPI, TGFA, THY1, TLR1, TMEM100, TMEM119, TMEM204, TNFRSF19, TNFRSF1A, UNC5A, UNC5D, VIM, VIPR1, VSTM2A	1.42	<0.001	<0.001
Receptor complex (GO:0043235)	ENG, GPR160, GPR37L1, INSRR, ITGB5, LIFR, LRP1B, NTRK3, P2RX3, PEX5L, PTH1R, TNFRSF1A, VDR, VIPR1	3.83	0.101	0.003
Synapse (GO:0045202)	ASIC1, CBLN4, CNTN2, DACT1, GABRA5, GABRB3, LGI1, MME, MYO7A, NLGN4X, NRCAM, PPFIA2, PRIMA1, RPH3A, SCGN, SDK2, SNCB, TENM2	3.46	0.026	<0.001

FDR, false discovery rate

Table 2. Selected genes with different expression levels in the FHTRα1-C380fsx387 regulated compared to FHTRα1 WT and -F397fsx406, and with known functions in neuronal growth and migration (the gene descriptions are extracted from GeneCards: www.genecards.org).

Gene symbol	Protein	Description
Guidance molecules		
SEMA3A	Semaphorin 3A	Protein can function as either a chemorepulsive (inhibiting outgrowth of axon), or a chemoattractive agent (stimulating the growth of axon)
SEMA3C	Semaphorin 3C	Functions as attractant for growing axons, and thereby plays an important role in axon growth and axon guidance
SLIT1	Slit guidance ligand 1	SLIT1 and SLIT2 together seem to be essential for midline guidance in the forebrain by acting as repulsive signal preventing inappropriate midline crossing by axons projecting from the olfactory bulb
EFNB2	Ephrin B2	Cell surface transmembrane ligand for Eph receptors which are crucial for migration, repulsion and adhesion during neuronal development
UNC5A	UNC-5 netrin receptor A	Protein belongs to a family of netrin-1 receptors thought to mediate the chemorepulsive effect of netrin-1 on specific axons
UNC5D	UNC-5 netrin receptor D	Receptor for the netrin NTN4. Plays a role in axon guidance by inhibit axon growth cones in the nervous system development upon ligand binding
Cell adhesion molecules		
NRCAM	Neuronal cell adhesion (Immunoglobulin superfamily, IgSF)	Involved in neuron-neuron adhesion and directional signal during axonal growth
CNTN4	Contactin 4 (Contactin family of immunoglobulin)	Function in neuronal network formation and plasticity
CNTNAP5	Contactin associated protein like 5 (Neurexin family)	Function as cell adhesion molecules in the vertebrate nervous system
THY1	Thy-1 cell surface antigen (IgSF superfamily)	Involved in cellular adhesion of the immune and nervous systems
PCDH1	Protocadherin 1 (Cadherin superfamily)	Involved in neural cell adhesion, suggesting a possible role in neuronal development
PCDH17	Protocadherin 17 (Cadherin superfamily)	Protein may involve in the cellular connections in the brain
FAT3	FAT atypical cadherin 3	May play a role in the interactions between neurites derived from specific subsets of neurons during development
ITGA1	Integrin subunit alpha 1 (integrin superfamily)	The protein heterodimerizes with the beta 1 subunit and involved in cell-cell adhesion
ITGA9	Integrin subunit alpha 9 (Integrin superfamily)	The protein heterodimerizes with the beta chain and mediates cell-cell and cell-matrix adhesion
ITGB5	Integrin subunit beta 5 (Integrin superfamily)	Combines with different alpha chains to form a variety of integrin heterodimers and participates in cell adhesion and cell surface mediates signaling
ASTN2	Astrotactin 2	Protein is expressed in the brain and may function in neuronal migration

Gene symbol	Protein	Description
Neurotrophic factors		
NGFR	Nerve growth factor receptor	Low affinity receptor which binds to multiple neurotrophic factors and regulates neuronal cell survival and cell death
NTRK3	Neurotrophic receptor tyrosine kinase 3	Binds to its ligand neurotropin 3 (NT-3) and involved in nervous system development
GFRA2	Glial-derived neurotrophic factor (GDNF) family receptor alpha 2	Encoded protein acts preferentially as a receptor for neurturin (NTN), potent neurotrophic factors for neuron survival and differentiation
Neuronal differentiation		
ASCL1	Achaete-Scute family bHLH transcription factor 1	Protein plays a role in the neuronal cell commitment and differentiation
NEUROG2	Neurogenin 2	Protein is expressed in neural progenitor cells within the developing central and peripheral nervous systems to specify a neuronal fate

Discussion

In this study, we evaluated the differences in the transcriptomes controlled by two TRα1 truncating mutants (C380fsx387 and F397fsx406) and WT TRα1 in a neuronal cell model (SH-SY5Y) in order to gain a better understanding of the differential effects of these mutations on the neurological phenotype of RTHα patients. The results showed that the transcriptomes of SH-SY5Y cells overexpressing FHTRα1-C380fsx387 and -F397fsx406 mutants were very different from the T3-stimulated but also the unstimulated transcriptome of WT TRα1. This suggests that the presence of these two mutants alters both baseline and T3-induced gene transcription. In addition, the transcriptomes of the two mutants were very different from each other, suggesting a differential effect of these two different mutations on gene transcription.

Previous studies showed that the phenotype of RTHα patients is mainly caused by the reduced T3 binding affinity of TRα1 mutants. However, patients that carry different TRα1 truncating mutations, all of which exhibited negligible T3 binding, display a striking variation in the cognitive phenotype. For instance, the patient who carries TRα1-C380fsx387 mutation was severely handicapped and unable to communicate at 12 years of age, suggesting severe cognitive impairment (17). Patients who carry TRα1-A382fsx388 and C392X mutations also had a low IQ score (IQ score 52 and 22, respectively) (15,16). In contrast, patients who carry TRα1-F397fsx406 and E403X mutations had borderline cognitive impairment (IQ score 90 and 70, respectively) (13-15). This suggests that other effects of the mutation that are independent from T3-binding can contribute to the phenotype as well (8,12,13,15-17,33). TRα1-C380fsx387 and -F397fsx406 were selected because of the marked differences in the

severity of the cognitive impairment in the patients harboring these mutations. In agreement with previous reports (13,17), both mutants had no response to T3 in luciferase experiments, confirming that T3 could not stimulate transcriptional activity for these mutants.

In SH-SY5Y/FHTRα1 WT cells, the expression of a substantial number of genes (5,688 genes) was regulated by T3 in contrast to SH-SY5Y/MCS controls cells (43 genes). The T3-induced response of WT receptor can be divided into two groups. The first group is a positive regulation in which the level of gene expression is increased in the presence of T3 (2,999 genes, 53%). The second group is a negative regulation in which the level of gene expression is decreased in the presence of T3 (2,689 genes, 47%). Interestingly, the number of genes in both groups is similar. The number of T3 negatively regulated genes in the brain varies (15-60%) between reports, depending on the cellular context and experimental technique (34-38). So far, the molecular mechanisms underlying the negative regulation by T3 have not yet been clearly established.

In contrast to the WT receptor, the transcriptomes regulated by FHTRα1-C380fsx387 and -F397fsx406 were not significantly altered by 10 nM T3 stimulation for any gene, which is in line with negligible T3 binding of these two mutants. Since we were interested in the differential effect of these two mutants on gene transcription, we then studied whether these mutants alter unstimulated gene expression compared to the WT receptor in a different way. The results indicate that the number of H-DE genes between SH-SY5Y/FHTRα1-C380fsx387 and WT cells was higher than that between -F397fsx406 and WT cells (888 vs. 471 genes). This finding suggests that the effect of these two mutants on gene expression is beyond their loss of affinity for T3. In addition, the much larger impact of the C380fsx387 mutant on unstimulated gene transcription compared to the F397fsx406 mutant likely contributes to the difference in the neurological phenotype of the patients.

We performed gene ontology (GO) term enrichment analysis to understand the functions of the genes that are differentially expressed between unstimulated SH-SY5Y/FHTRα1-C380fsx387 vs. -F397fsx406 cells. We only selected the H-DE genes that had at least a 4-fold difference in expression between the two mutants for the analysis since a difference in expression of these genes is likely to have an impact on the difference in phenotype of patients. The results showed that approximately 50% of the selected genes were significantly enriched for at least one GO term. Most of the significant terms were related to neurons (axon, dendrite, synapse) and physiology of the neurons (axon guidance, axon fasciculation, cell adhesion, calcium ion binding, and cell junction). These findings further support the hypothesis that a differential effect of the C380fsx387 and F397fsx406 mutants on gene expression may disturb the pathways that are critical for the brain and neurons.

One of the most significant terms in our GO analysis is axon guidance. Genes enriched for this term encode proteins that act as extracellular guidance cues for neuronal growth and migration. These cues can either attract or repulse axon growth. *SEMA3A* and *SEMA3C* encode Semaphorin 3A and 3C that bind to the plexin and neuropillin receptor and

inhibit axon growth (39-42). *SLIT1* encodes Slit1 that signals through Roundabout (Robo) family receptors and controls midline guidance of axons (42-45). *EFNB2* encodes Ephrin B2, which is a membrane-bound ligand that binds to EphB tyrosine kinase receptors, and mediates cell to cell communication and neuronal development (42,46-48). *UNC5A* and *UNC5D* encode UNC-5 homolog proteins A and D which function as receptors for axonal attractive molecule, Netrin (42,49,50). In addition to the axonal growth, these cues are involved in dendrite development (51,52) and cortical migration of the neurons (53). By responding to appropriate signals, the neurons grow into the correct paths, which leads to proper neurodevelopment. Since the expression of these genes in SH-SY5Y/ FHTRα1-C380fsx387 cells was significantly different from both SH-SY5Y/ FHTRα1 WT and -F397fsx406 cells, it is likely that these genes may have contributed to the more severe neurodevelopmental impairment found in the patient carrying the C380fsx387 mutation.

Apart from the genes that were enriched for GO terms, the expression of *ASCL1* and *NEUROG2* was also markedly different in SH-SY5Y/FHTRα1-C380fsx387 cells compared to SH-SY5Y/FHTRα1 WT and -FHTRα1-F397fsx406 cells (Figure 6). These genes encode Achaete-scute homolog 1 (ASCL1) and Neurogenin 2 (NEUROG2), respectively, which are master regulators of neuronal differentiation. Many studies using murine models suggest that in cortical brain development, Neurog2 expression commits progenitor cells to become excitatory (glutamatergic) neurons, whereas Ascl1 expression commits cells to become inhibitory (GABAergic) neurons (54-58). In addition, highly expressed Ascl1 keeps neuron progenitor cells in the proliferative phase rather than enter the differentiation process (55). Therefore, the relatively high expression of the *ASCL1* and low expression of the *NEUROG2* in SH-SY5Y/ FHTRα1-C380fsx387 cells (Figure 6) are likely to affect progenitor cell differentiation and the balance between excitatory and inhibitory neurons, which may relate to the severe cognitive impairment found in the TRα1-C380fsx387 patient.

Although our study showed that TRα1-C380fsx387 and TRα1-F397fsx406 have a differential effect on gene transcription, the underlying mechanism explaining this differential effect remains unclear. It has been shown that the C-terminal region of TRα1 protein is important for the interaction with corepressor and coactivator proteins (59-62). Since the location of the frameshift and premature stop codon of TRα1-C380fsx387 is proximal to that of TRα1-F397fsx406 mutant, the C-terminal region of the TRα1-C380fsx387 mutant is likely more distorted. The C380fsx387 mutation alters both Helix [H] 11 and 12, whereas the F397fsx406 mutation only alters H12. The more prominent structural changes in the TRα1-C380fsx387 mutant might result in more exposure to the corepressor docking surface than in case of the TRα1-F397fsx406 mutant. This would allow corepressor proteins to bind stronger to the TRα1-C380fsx387 mutant than to the TRα1-F397fsx406 mutant and lead to stronger gene repression. Alternatively, since TRs can associate with and be regulated by multiple coregulatory proteins, different binding surfaces of the mutants may result in the recruitment of a different repertoire of proteins that ultimately affects the expression of target genes.

It is important to emphasize that our experiments were performed by overexpressing WT or mutant TRα1 in SH-SY5Y cells, which creates a non-physiologic level of TRα1 expression. A high level of mutant TRα1 in the cells against a background of low levels of endogenous WT TRα1 expression may not mimic the actual situation in which both WT and mutant *THRA* alleles are expressed at equal levels. Therefore, the effect of the mutants may be under or overestimated in our system. Although the lentiviral transduction with subsequent clonal selection is widely used to create a stable cell line of interest, it has a (tiny) chance that viral DNA that integrates into the cell genome disrupts a vital region of the genome, which may have complicated the result. Therefore, experiments in more physiologic systems such as CRISPR-Cas9 genome editing, primary cells derived from patients, or knock-in animals are needed to independently confirm our findings. Last, since neuronal development is a highly dynamic process, data from one snap-shot in a neuroblastoma cell line may represent only a small part of the whole neurodevelopmental process.

In summary, the transcriptome regulated by the two TRα1 truncating mutants, TRα1-C380fsx387 and -F397fsx406, in SH-SY5Y cells are widely different. Unstimulated gene expression controlled by the TRα1-C380fsx387 mutant is more different from WT than that controlled by the TRα1-F397fsx406 mutant. Interestingly, this involves many genes that have a vital role in neuronal development. These findings may, at least in part, explain the more severe neurological phenotype found in the patient carrying the TRα1-C380fsx387 mutation.

Acknowledgement

This work is supported by Zon-MWTOP Grant 91212044 and an Erasmus MC Medical Research Advisory Committee (MRACE) grant (RPP, MEM), and Chiang Mai University (KW).

Disclosure

The authors have nothing to disclose.

References

1. Bernal J. Thyroid hormone regulated genes in cerebral cortex development. *J Endocrinol.* 2017;**232**(2):R83-R97.
2. Bernal J. Thyroid hormone receptors in brain development and function. *Nat Clin Pract Endocrinol Metab.* 2007;**3**(3):249-259.
3. Gothie JD, Demeneix B, Remaud S. Comparative approaches to understanding thyroid hormone regulation of neurogenesis. *Mol Cell Endocrinol.* 2017;**459**:104-115.
4. Wallis K, Dudazy S, van Hogerlinden M, Nordstrom K, Mittag J, Vennstrom B. The thyroid hormone receptor alpha1 protein is expressed in embryonic postmitotic neurons and persists in most adult neurons. *Mol Endocrinol.* 2010;**24**(10):1904-1916.
5. Mellstrom B, Naranjo JR, Santos A, Gonzalez AM, Bernal J. Independent expression of the alpha and beta c-erbA genes in developing rat brain. *Mol Endocrinol.* 1991;**5**(9):1339-1350.
6. Bradley DJ, Towle HC, Young WS, 3rd. Spatial and temporal expression of alpha- and beta-thyroid hormone receptor mRNAs, including the beta 2-subtype, in the developing mammalian nervous system. *The Journal of neuroscience : the official journal of the Society for Neuroscience.* 1992;**12**(6):2288-2302.
7. Flamant F, Gauthier K, Richard S. Genetic Investigation of Thyroid Hormone Receptor Function in the Developing and Adult Brain. *Curr Top Dev Biol.* 2017;**125**:303-335.
8. van Gucht ALM, Moran C, Meima ME, Visser WE, Chatterjee K, Visser TJ, Peeters RP. Resistance to Thyroid Hormone due to Heterozygous Mutations in Thyroid Hormone Receptor Alpha. *Curr Top Dev Biol.* 2017;**125**:337-355.
9. Singh BK, Yen PM. A clinician's guide to understanding resistance to thyroid hormone due to receptor mutations in the TRalpha and TRbeta isoforms. *Clin Diabetes Endocrinol.* 2017;**3**:8.
10. Moran C, Chatterjee K. Resistance to Thyroid Hormone alpha-Emerging Definition of a Disorder of Thyroid Hormone Action. *J Clin Endocrinol Metab.* 2016;**101**(7):2636-2639.
11. Moran C, Chatterjee K. Resistance to thyroid hormone due to defective thyroid receptor alpha. *Best Pract Res Clin Endocrinol Metab.* 2015;**29**(4):647-657.
12. Bochukova E, Schoenmakers N, Agostini M, Schoenmakers E, Rajanayagam O, Keogh JM, Henning E, Reinemund J, Gevers E, Sarri M, Downes K, Offiah A, Albanese A, Halsall D, Schwabe JW, Bain M, Lindley K, Muntoni F, Vargha-Khadem F, Dattani M, Farooqi IS, Gurnell M, Chatterjee K. A mutation in the thyroid hormone receptor alpha gene. *N Engl J Med.* 2012;**366**(3):243-249.
13. van Mullem A, van Heerebeek R, Chrysis D, Visser E, Medici M, Andrikoula M, Tsatsoulis A, Peeters R, Visser TJ. Clinical phenotype and mutant TRalpha1. *N Engl J Med.* 2012;**366**(15):1451-1453.
14. van Mullem AA, Chrysis D, Eythimiadou A, Chroni E, Tsatsoulis A, de Rijke YB, Visser WE, Visser TJ, Peeters RP. Clinical phenotype of a new type of thyroid hormone resistance caused by a mutation of the TRalpha1 receptor: consequences of LT4 treatment. *The Journal of clinical endocrinology and metabolism.* 2013;**98**(7):3029-3038.
15. Tylki-Szymanska A, Acuna-Hidalgo R, Krajewska-Walasek M, Lecka-Ambroziak A, Steehouwer M, Gilissen C, Brunner HG, Jurecka A, Rozdzynska-Swiatkowska A, Hoischen A, Chrzanowska KH. Thyroid hormone resistance syndrome due to mutations in the thyroid hormone receptor alpha gene (THRA). *J Med Genet.* 2015;**52**(5):312-316.
16. Moran C, Schoenmakers N, Agostini M, Schoenmakers E, Offiah A, Kydd A, Kahaly G, Mohr-Kahaly S, Rajanayagam O, Lyons G, Wareham N, Halsall D, Dattani M, Hughes S, Gurnell M, Park SM, Chatterjee K. An adult female with resistance to thyroid hormone mediated by defective thyroid hormone receptor alpha. *J Clin Endocrinol Metab.* 2013;**98**(11):4254-4261.
17. Demir K, van Gucht AL, Buyukinan M, Catli G, Ayhan Y, Bas VN, Dundar B, Ozkan B, Meima ME, Visser WE, Peeters RP, Visser TJ. Diverse Genotypes and Phenotypes of Three Novel Thyroid Hormone Receptor-alpha Mutations. *The Journal of clinical endocrinology and metabolism.* 2016;**101**(8):2945-2954.

18. Stampfer M, Beck-Wodl S, RieB A, Haack T. Most severe case of thyroid-alpha-receptor deficiency in a female patient with severe growth and mental retardation, macrocephaly, pubertas tarda and dysgerminoma. Poster presented at The European Society of Human Genetics 28 May, 2017;P08.65A (abstract).

19. Sun H, Wu H, Xie R, Wang F, Chen T, Chen X, Wang X, Flamant F, Chen L. New Case of Thyroid Hormone Resistance alpha Caused by a Mutation of THRA /TRalpha1. *J Endocr Soc.* 2019;**3**(3):665-669.

20. Moran C, Agostini M, Visser WE, Schoenmakers E, Schoenmakers N, Offiah AC, Poole K, Rajanayagam O, Lyons G, Halsall D, Gurnell M, Chrysis D, Efthymiadou A, Buchanan C, Aylwin S, Chatterjee KK. Resistance to thyroid hormone caused by a mutation in thyroid hormone receptor (TR)alpha1 and TRalpha2: clinical, biochemical, and genetic analyses of three related patients. *Lancet Diabetes Endocrinol.* 2014;**2**(8):619-626.

21. Espiard S, Savagner F, Flamant F, Vlaeminck-Guillem V, Guyot R, Munier M, d'Herbomez M, Bourguet W, Pinto G, Rose C, Rodien P, Wemeau JL. A Novel Mutation in THRA Gene Associated With an Atypical Phenotype of Resistance to Thyroid Hormone. *J Clin Endocrinol Metab.* 2015;**100**(8):2841-2848.

22. van Gucht AL, Meima ME, Zwaveling-Soonawala N, Visser WE, Fliers E, Wennink JM, Henny C, Visser TJ, Peeters RP, van Trotsenburg AS. Resistance to Thyroid Hormone Alpha in an 18-Month-Old Girl: Clinical, Therapeutic, and Molecular Characteristics. *Thyroid.* 2016;**26**(3):338-346.

23. Moran C, Agostini M, McGowan A, Schoenmakers E, Fairall L, Lyons G, Rajanayagam O, Watson L, Offiah A, Barton J, Price S, Schwabe J, Chatterjee K. Contrasting Phenotypes in Resistance to Thyroid Hormone Alpha Correlate with Divergent Properties of Thyroid Hormone Receptor alpha1 Mutant Proteins. *Thyroid.* 2017;**27**(7):973-982.

24. Kalikiri MK, Mamidala MP, Rao AN, Rajesh V. Analysis and functional characterization of sequence variations in ligand binding domain of thyroid hormone receptors in autism spectrum disorder (ASD) patients. *Autism Res.* 2017;**10**(12):1919-1928.

25. Wejaphikul K, Groeneweg S, Hilhorst-Hofstee Y, Chatterjee VK, Peeters RP, Meima ME, Visser WE. Insight into molecular determinants of T3 vs. T4 recognition from mutations in thyroid hormone receptor alpha and beta. *J Clin Endocrinol Metab.* 2019;**104**(8):3491-3500.

26. Korkmaz O, Ozen S, Ozdemir TR, Goksen D, Darcan S. A novel thyroid hormone receptor alpha gene mutation, clinic characteristics, and follow-up findings in a patient with thyroid hormone resistance. *Hormones (Athens).* 2019;**10.1007/s42000-019-00094-9**.

27. Yuen RK, Thiruvahindrapuram B, Merico D, Walker S, Tammimies K, Hoang N, Chrysler C, Nalpathamkalam T, Pellecchia G, Liu Y, Gazzellone MJ, D'Abate L, Deneault E, Howe JL, Liu RS, Thompson A, Zarrei M, Uddin M, Marshall CR, Ring RH, Zwaigenbaum L, Ray PN, Weksberg R, Carter MT, Fernandez BA, Roberts W, Szatmari P, Scherer SW. Whole-genome sequencing of quartet families with autism spectrum disorder. *Nat Med.* 2015;**21**(2):185-191.

28. Wejaphikul K, Groeneweg S, Dejkhamron P, Unachak K, Visser WE, Chatterjee VK, Visser TJ, Meima ME, Peeters RP. Role of Leucine 341 in Thyroid Hormone Receptor Beta Revealed by a Novel Mutation Causing Thyroid Hormone Resistance. *Thyroid.* 2018;**28**(12):1723-1726.

29. Love MI, Huber W, Anders S. Moderated estimation of fold change and dispersion for RNA-seq data with DESeq2. *Genome Biol.* 2014;**15**(12):550.

30. Bernal J, Morte B. Expression Analysis of Genes Regulated by Thyroid Hormone in Neural Cells. *Methods Mol Biol.* 2018;**1801**:17-28.

31. Chatonnet F, Flamant F, Morte B. A temporary compendium of thyroid hormone target genes in brain. *Biochim Biophys Acta.* 2015;**1849**(2):122-129.

32. Gil-Ibanez P, Bernal J, Morte B. Thyroid hormone regulation of gene expression in primary cerebrocortical cells: role of thyroid hormone receptor subtypes and interactions with retinoic acid and glucocorticoids. *PLoS One.* 2014;**9**(3):e91692.

33. Huang T, Wang T, Heianza Y, Zheng Y, Sun D, Kang JH, Pasquale LR, Rimm EB, Manson JE, Hu FB, Qi L. Habitual consumption of long-chain n-3 PUFAs and fish attenuates genetically

associated long-term weight gain. *The American journal of clinical nutrition.* 2019;**109**(3):665-673.

34. Chatonnet F, Guyot R, Benoit G, Flamant F. Genome-wide analysis of thyroid hormone receptors shared and specific functions in neural cells. *Proceedings of the National Academy of Sciences of the United States of America.* 2013;**110**(8):E766-775.
35. Diez D, Grijota-Martinez C, Agretti P, De Marco G, Tonacchera M, Pinchera A, de Escobar GM, Bernal J, Morte B. Thyroid hormone action in the adult brain: gene expression profiling of the effects of single and multiple doses of triiodo-L-thyronine in the rat striatum. *Endocrinology.* 2008;**149**(8):3989-4000.
36. Miller LD, McPhie P, Suzuki H, Kato Y, Liu ET, Cheng SY. Multi-tissue gene-expression analysis in a mouse model of thyroid hormone resistance. *Genome Biol.* 2004;**5**(5):R31.
37. Morte B, Diez D, Auso E, Belinchon MM, Gil-Ibanez P, Grijota-Martinez C, Navarro D, de Escobar GM, Berbel P, Bernal J. Thyroid hormone regulation of gene expression in the developing rat fetal cerebral cortex: prominent role of the Ca2+/calmodulin-dependent protein kinase IV pathway. *Endocrinology.* 2010;**151**(2):810-820.
38. Gil-Ibanez P, Garcia-Garcia F, Dopazo J, Bernal J, Morte B. Global Transcriptome Analysis of Primary Cerebrocortical Cells: Identification of Genes Regulated by Triiodothyronine in Specific Cell Types. *Cereb Cortex.* 2017;**27**(1):706-717.
39. Jongbloets BC, Pasterkamp RJ. Semaphorin signalling during development. *Development.* 2014;**141**(17):3292-3297.
40. Mann F, Chauvet S, Rougon G. Semaphorins in development and adult brain: Implication for neurological diseases. *Prog Neurobiol.* 2007;**82**(2):57-79.
41. Masuda T, Taniguchi M. Contribution of semaphorins to the formation of the peripheral nervous system in higher vertebrates. *Cell Adh Migr.* 2016;**10**(6):593-603.
42. Dickson BJ. Molecular mechanisms of axon guidance. *Science.* 2002;**298**(5600):1959-1964.
43. Blockus H, Chedotal A. Slit-Robo signaling. *Development.* 2016;**143**(17):3037-3044.
44. Andrews WD, Barber M, Parnavelas JG. Slit-Robo interactions during cortical development. *J Anat.* 2007;**211**(2):188-198.
45. Bagri A, Marin O, Plump AS, Mak J, Pleasure SJ, Rubenstein JL, Tessier-Lavigne M. Slit proteins prevent midline crossing and determine the dorsoventral position of major axonal pathways in the mammalian forebrain. *Neuron.* 2002;**33**(2):233-248.
46. Kania A, Klein R. Mechanisms of ephrin-Eph signalling in development, physiology and disease. *Nat Rev Mol Cell Biol.* 2016;**17**(4):240-256.
47. Singhal J, Nagaprashantha LD, Vatsyayan R, Ashutosh, Awasthi S, Singhal SS. Didymin induces apoptosis by inhibiting N-Myc and upregulating RKIP in neuroblastoma. *Cancer Prev Res (Phila).* 2012;**5**(3):473-483.
48. Niethamer TK, Bush JO. Getting direction(s): The Eph/ephrin signaling system in cell positioning. *Dev Biol.* 2019;**447**(1):42-57.
49. Rajasekharan S, Kennedy TE. The netrin protein family. *Genome Biol.* 2009;**10**(9):239.
50. Boyer NP, Gupton SL. Revisiting Netrin-1: One Who Guides (Axons). *Front Cell Neurosci.* 2018;**12**:221.
51. Lanoue V, Cooper HM. Branching mechanisms shaping dendrite architecture. *Dev Biol.* 2019;**451**(1):16-24.
52. Goshima Y, Yamashita N, Nakamura F, Sasaki Y. Regulation of dendritic development by semaphorin 3A through novel intracellular remote signaling. *Cell Adh Migr.* 2016;**10**(6):627-640.
53. Ayala R, Shu T, Tsai LH. Trekking across the brain: the journey of neuronal migration. *Cell.* 2007;**128**(1):29-43.
54. Chouchane M, Costa MR. Instructing neuronal identity during CNS development and astroglial-lineage reprogramming: Roles of NEUROG2 and ASCL1. *Brain Res.* 2019;**1705**:66-74.
55. Wilkinson G, Dennis D, Schuurmans C. Proneural genes in neocortical development.

Neuroscience. 2013;**253**:256-273.

56. Guillemot F, Hassan BA. Beyond proneural: emerging functions and regulations of proneural proteins. *Curr Opin Neurobiol.* 2017;**42**:93-101.
57. Schuurmans C, Armant O, Nieto M, Stenman JM, Britz O, Klenin N, Brown C, Langevin LM, Seibt J, Tang H, Cunningham JM, Dyck R, Walsh C, Campbell K, Polleux F, Guillemot F. Sequential phases of cortical specification involve Neurogenin-dependent and -independent pathways. *EMBO J.* 2004;**23**(14):2892-2902.
58. Berninger B, Guillemot F, Gotz M. Directing neurotransmitter identity of neurones derived from expanded adult neural stem cells. *Eur J Neurosci.* 2007;**25**(9):2581-2590.
59. Tagami T, Gu WX, Peairs PT, West BL, Jameson JL. A novel natural mutation in the thyroid hormone receptor defines a dual functional domain that exchanges nuclear receptor corepressors and coactivators. *Mol Endocrinol.* 1998;**12**(12):1888-1902.
60. Rosen MD, Privalsky ML. Thyroid hormone receptor mutations found in renal clear cell carcinomas alter corepressor release and reveal helix 12 as key determinant of corepressor specificity. *Mol Endocrinol.* 2009;**23**(8):1183-1192.
61. Marimuthu A, Feng W, Tagami T, Nguyen H, Jameson JL, Fletterick RJ, Baxter JD, West BL. TR surfaces and conformations required to bind nuclear receptor corepressor. *Mol Endocrinol.* 2002;**16**(2):271-286.
62. Wu SY, Cohen RN, Simsek E, Senses DA, Yar NE, Grasberger H, Noel J, Refetoff S, Weiss RE. A novel thyroid hormone receptor-beta mutation that fails to bind nuclear receptor corepressor in a patient as an apparent cause of severe, predominantly pituitary resistance to thyroid hormone. *J Clin Endocrinol Metab.* 2006;**91**(5):1887-1895.

Supplementary Materials

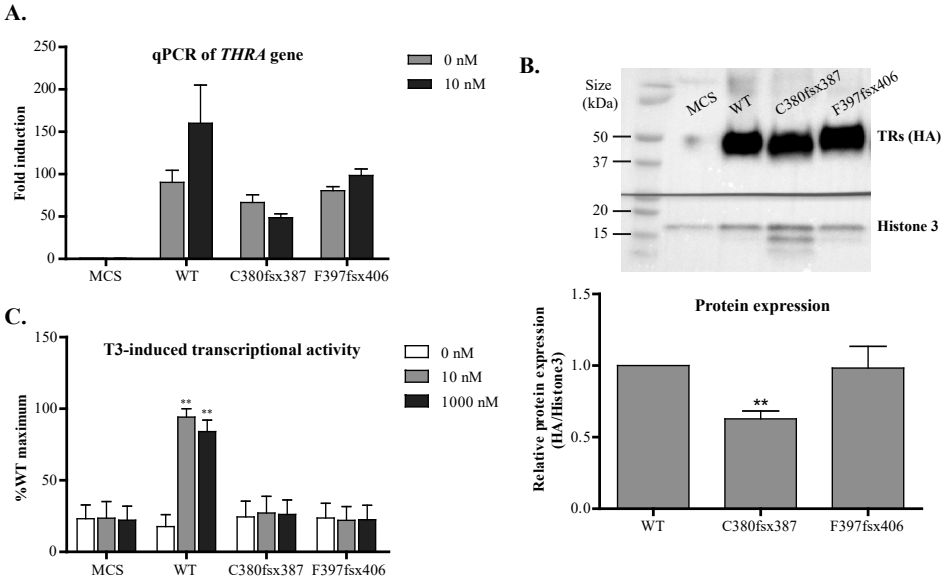

Supplementary Figure S1. (A) The qPCR analysis shows a high expression of the *THRA* in all three FHTRα1 expressing cell lines (SH-SY5Y/FHTRα1 WT, -C380fsx387, and -F397fsx406), confirming the success of FHTRα1 transduction. (B) The FHTRα1 protein expression (detected by 1:1,000 dilution of a HA antibody) showed that all three FHTRα1 are expressed in the cells with a slightly lower expression level for FHTRα1-C380fsx387 than for WT and -F397fsx406. (Relative protein expression (band intensity) of three independent blots is quantified by ImageJ program and showed as mean ± SEM, One-sample t-test compared to WT **p<0.01.) (C) The T3-induced transcriptional activity of FHTRα1 WT is increased in the presence of T3. In contrast, the two truncating mutants showed no response to T3-stimulation, indicating a complete loss of T3-induced transcriptional activity (data are shown as mean ± SEM of three independent luciferase assay experiments performed in triplicates, Student's t-test compared to 0 nM T3 **p<0.01).

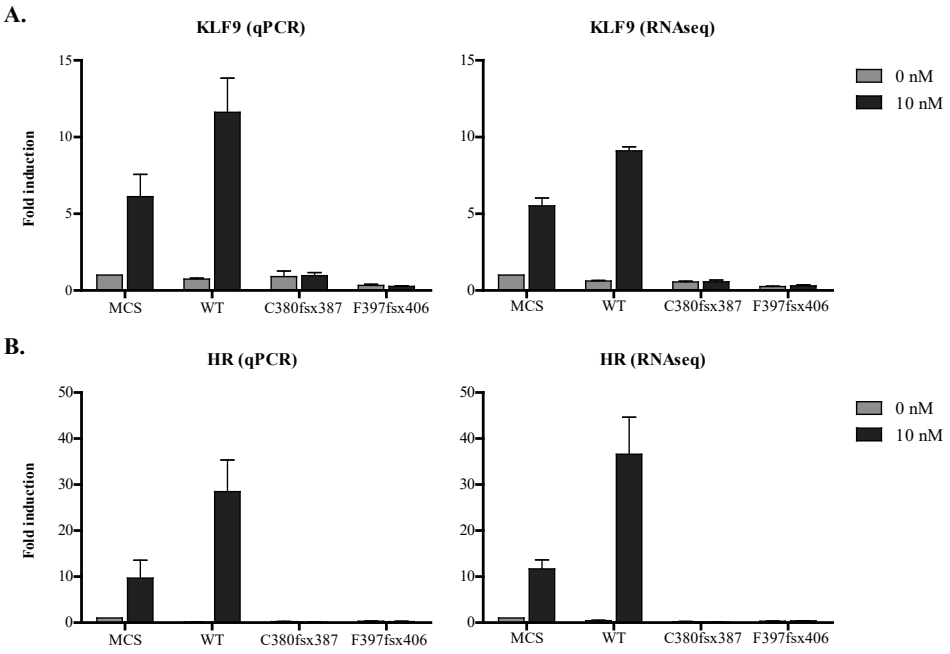

Supplementary Figure S2. qRT-PCR analysis (left panel) and RNA sequencing (right panel) of the (A) *KLF9* and (B) *HR* (Hairless) show a similar pattern between the two methods. The data are shown as mean ± SEM of the fold induction (adjusted MCS 0 nM T3 = 1).